All-Electrical Control of Single Ion Spins in a Semiconductor

Jian-Ming Tang,[1] Jeremy Levy,[2] and Michael E. Flatté[1]

[1]*Department of Physics and Astronomy, University of Iowa, Iowa City, Iowa 52242-1479, USA*
[2]*Department of Physics and Astronomy, University of Pittsburgh, Pittsburgh, Pennsylvania 15260, USA*

(Received 9 February 2006; published 5 September 2006; publisher error corrected 6 September 2006)

We propose a method for all-electrical manipulation of single ion spins substituted into a semiconductor. Mn ions with a bound hole in GaAs form a natural example. Direct electrical manipulation of the ion spin is possible, because electric fields manipulate the orbital wave function of the hole, and through the spin-orbit coupling the spin is reoriented as well. Coupling ion spins can be achieved using gates to control the size of the hole wave function. Coherent manipulation of ionic spins may find applications in high-density storage and in scalable coherent or quantum information processing.

DOI: 10.1103/PhysRevLett.97.106803 PACS numbers: 73.20.−r, 03.67.Lx, 75.75.+a, 76.30.Da

Observing magnetic resonance between different spin states of nuclei or electrons is a technique widely used in many imaging and spectroscopic applications. Sensitivity sufficient to measure the fluctuation of a single spin has been demonstrated using magnetic resonance force microscopy [1], noise spectroscopy [2], optical spectroscopy [3,4], scanning tunneling microscopy (STM) [5–7], and quantum point contact conductivity [8]. The potential also exists to determine the spin state [2,4,8,9]. Controlling a single spin, in addition to monitoring it, is highly desirable for building future spin-based devices, is essential for quantum computation, and should permit the direct exploration of fundamental aspects of quantum dynamics in a solid state environment [10–13]. Proposed schemes to control a single spin in a solid state environment rely on either magnetic resonance [14,15] or optical manipulation [16–18], and there has been progress towards replacing magnetic control fields with the spin-orbit interaction [19,20] or the exchange interaction [21,22].

Ionic spin states in solids have several attractive characteristics for fundamental studies of spin dynamics and for spin-based devices. Every ion embedded in a solid is identical to every other such ion. Thus, an ionic spin system can be as uniform as a nuclear spin system but also can permit spin manipulation on short time scales as in a quantum dot spin system. Controlling ionic single spins without any magnetic fields, using techniques in which electric fields play the typical role of magnetic fields, may therefore provide a path to high-density scalable spin-based electronics. For example, the control of ionic spin states can be used to produce highly spin-selective and spin-dependent tunneling currents in nanoscale electrical devices or to realize quantum computation. Manipulation of individual spins that are constituents of interacting spin clusters also opens up the capability to explore the fundamental dynamics of frustrated spin systems and other correlated spin systems.

Here we propose an all-electrical scheme for ionic spin manipulation in which the role of magnetic fields in traditional electron spin resonance (ESR) is replaced by electric fields. In conventional ESR, the energy splitting between different spin states and the couplings between them are controlled by magnetic fields, because an electric field does not directly couple to the electron's spin. In a semiconductor crystal with tetrahedral symmetry and spin-orbit interaction (such as GaAs), a $J = 1$ ion spin (such as that of Mn in GaAs) will be triply degenerate; however, the energy splittings and the couplings between these states depend *linearly* on the *electric field* strength, allowing rapid all-electrical control. Thus, all operations performed with magnetic fields in traditional ESR can be performed with electrical techniques.

A specific proposed setup for manipulating a single ion spin is shown in Fig. 1. Tip-induced placement of single Mn ions substituted for Ga in a GaAs sample has been demonstrated experimentally [23]. Two gates are configured to apply an electric field along the [001] axis. The STM tip serves as the third gate for spin manipulation and as a contact for initialization and detection. Taking advantage of the (110) natural cleavage plane (which lacks surface states), the applied electric field is confined in the

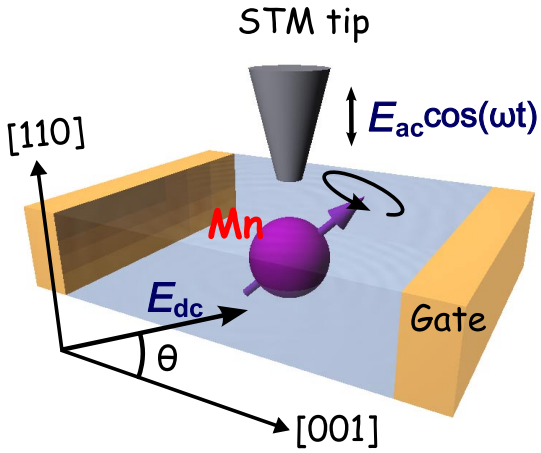

FIG. 1 (color online). Proposed configuration for the electric resonances of a single Mn dopant in GaAs. A dc electric field $\mathbf{E}_{dc}$ is applied via the electrical gates and the STM tip. The resonance is driven by an additional small ac field.

$(1\bar{1}0)$ plane and the orientation is specified by the angle θ from the [001] axis.

An isolated Mn atom has a half-filled $3d$ shell and the spins of all five $3d$ electrons are aligned (Hund's rule) to form a $S = 5/2$ ground state. In GaAs, a hole in the valence band compensates for the differing valences of Mn and Ga. We describe the core spin-valence hole dynamics with the following effective spin Hamiltonian:

$$\mathcal{H}_{\text{spin}} = \alpha \mathbf{S} \cdot \mathbf{s} + \beta \boldsymbol{l} \cdot \mathbf{s}, \tag{1}$$

where $\boldsymbol{l}$ and $\mathbf{s}$ are the orbital angular momentum ($l = 1$) and the spin of the bound hole, respectively. Our tight-binding calculations [24] estimate the exchange coupling α and the spin-orbit coupling β to be about 300 and -80 meV, respectively. The exchange interaction binds the valence hole with spin antiparallel to the Mn core spin with a binding energy of 113 meV [25]. The spin-orbit interaction in GaAs configures the orbital angular momentum of the hole parallel to its spin. The total angular momentum of the (Mn core + hole) complex is $\mathbf{J} = \mathbf{S} + \boldsymbol{l} + \mathbf{s}$, and the ground state of this complex has $J = 1$ [26] (both $\boldsymbol{l}$ and $\mathbf{s}$ are antiparallel to $\mathbf{S}$), confirmed via ESR [26]. Our proposals for spin control involve energy scales smaller than α or β, so only the lowest energy multiplet with $J = 1$ is of interest here.

The degeneracy of the $J = 1$ Mn ion can be substantially split by external electric fields, and the eigenstates depend strongly on the electric field direction. This will be the source of both state splitting (analogous to the static magnetic field in traditional ESR) and state coupling (analogous to the oscillating perpendicular magnetic field in traditional ESR). We find the following electric-field-dependent Hamiltonian:

$$\mathcal{H}_I(\mathbf{E}) = \gamma[E_x(J_y J_z + J_z J_y) + \text{c.p.}], \tag{2}$$

where $\mathbf{E}$ is an electric field, c.p. stands for cyclic permutation, and $\{x, y, z\}$ stand for the 3 major axes of the cubic crystal. Note that this Hamiltonian does not break time-reversal symmetry, for the angular momentum operators $\mathbf{J}$ always appear in pairs. We calculate, using the probability densities of the hole state found in our tight-binding calculations and first-order perturbation theory, $\gamma = 6.4 \times 10^{-30}$ C m, corresponding to $\gamma E = 160$ μeV for $E = 40$ kV/cm. This exceptionally large splitting is equivalent to that generated by applying a 1 T magnetic field using the measured g factor [26], 2.77. The linear dependence on electric field, critical to producing a large splitting, originates from the lack of inversion symmetry of the substituted ion in a tetrahedral host. The energy splittings from an electric field applied to bound states at inversion-symmetric sites in crystals, or electrons bound in atoms or ions in vacuum, would depend quadratically on the electric field and would be correspondingly much smaller. The other essential element causing this large splitting is the large (~ 10 Å) Bohr radius of the bound valence hole [24,27]. Recent progress in theory and scanning tunneling microscopy of Mn dopants in III–V semiconductors has confirmed the large spatial extent of the bound hole wave function [23,24,27,28]. Thus, the response of the Mn wave function to electric fields is substantial compared to other ion levels associated with transition-metal (magnetic) dopants.

In the basis $|X\rangle$, $|Y\rangle$, and $|Z\rangle$, defined by $J_\alpha|\alpha\rangle = 0$, the Hamiltonian can be written as

$$\mathcal{H}_I(\mathbf{E}) = -\gamma E \begin{pmatrix} 0 & \hat{E}_z & \hat{E}_y \\ \hat{E}_z & 0 & \hat{E}_x \\ \hat{E}_y & \hat{E}_x & 0 \end{pmatrix}. \tag{3}$$

The energy eigenvalues in units of γE are the roots of the characteristic polynomial

$$x^3 - x + 2\eta = 0, \tag{4}$$

where $\eta = \hat{E}_x \hat{E}_y \hat{E}_z$. A static electric field $\mathbf{E}_{\text{dc}}$ splits all three eigenstates in energy except when the field is in the [111] direction (or equivalent), for which two of the eigenstates remain degenerate.

The energies of the three states are $\xi_1 = (-\cos\theta - \sqrt{4 - 3\cos^2\theta})/2$, $\xi_2 = (-\cos\theta + \sqrt{4 - 3\cos^2\theta})/2$, and $\xi_3 = \cos\theta$, shown by the solid, dashed, and dotted curves, respectively, in Fig. 2(a). The eigenstate $|\xi_3\rangle = (|X\rangle - |Y\rangle)/\sqrt{2}$ is independent of θ. The independence of $|\xi_3\rangle$ from $\mathbf{E}$ (in this geometry) motivates us to define a pseudospin 1/2 constructed from the other two states, $|\xi_1\rangle$ and $|\xi_2\rangle$. These eigenstates can be written as $|\xi_1\rangle = (\sin\Theta/\sqrt{2}, \sin\Theta/\sqrt{2}, \cos\Theta)$ and $|\xi_2\rangle = (-\cos\Theta/\sqrt{2}, -\cos\Theta/\sqrt{2}, \sin\Theta)$, where Θ is the angle between $|\xi_1\rangle$ and the $|Z\rangle$ basis [Fig. 2(b)]. Note that all

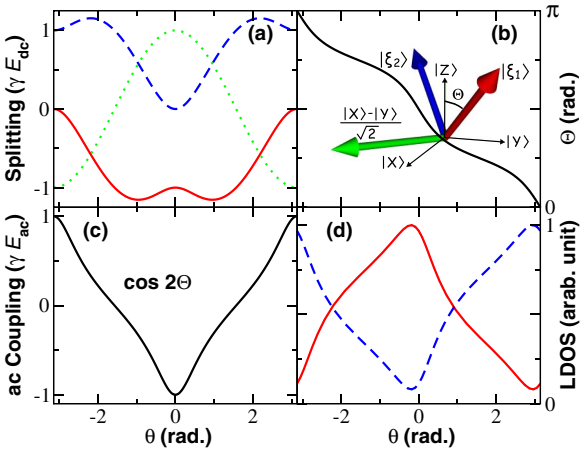

FIG. 2 (color online). The ionic spin system as a function of the dc field orientation. (a) The energies of the $J = 1$ states ξ_1 (solid line), ξ_2 (dashed line), and ξ_3 (dotted line). (b) The corresponding eigenvectors parametrized by the angle Θ. (c) The coupling between $|\xi_1\rangle$ and $|\xi_2\rangle$ due to the ac field. (d) The scaled LDOS of the two possible final states $|\xi_1\rangle$ (solid line) and $|\xi_2\rangle$ (dashed line) probed four monoatomic layers directly above the Mn dopant.

of the eigenvectors are real because of time-reversal symmetry.

Preparation of the initial pseudospin state is achieved by applying an electric field to split the state energies and allowing the hole to relax into the ground state. The electric field from the STM tip locally bends the bands of the semiconductor and permits ionization of the bound hole; this has been demonstrated for Mn in GaAs [27,29]. Rapid initialization of a high purity pseudospin state can be achieved by using the local band bending effect to move the two higher-energy levels (ξ_2, ξ_3) to the position shown in Fig. 3(a), so a hole in those states would ionize and be replaced by a hole in the lowest energy state ($|\xi_1\rangle$). At a temperature of 0.5 K and a dc field of 100 kV/cm, the occupation of the next highest state ($|\xi_2\rangle$) would be less than 10^{-4}. We have chosen $\mathbf{E}_{\rm dc}$ such that $|\theta| < (\pi - \tan^{-1}\sqrt{2})$, so that $|\xi_1\rangle$ (not $|\xi_3\rangle$) is the ground state [see Fig. 2(a)]. Band bending also changes the effective radius of the bound hole wave function; gate voltages applied at the surface could thus control the coupling of two bound hole states in an analogous way to the approaches in Refs. [14,15] for quantum dots and donor states.

In order to manipulate the initialized spins, the tip-sample bias should be increased adiabatically [slower than $\hbar/(\gamma E_{\rm dc})$] to bring all three levels into the semiconductor's energy gap [see Fig. 3(b)]. This shift with bias is described for Mn in p-doped GaAs in Ref. [27]. The bias voltage has to be maintained below the critical value at which electrons start to tunnel directly through these levels, so that the transitions between these states remain coherent. Spin resonance can now be driven by applying a small oscillating electric field $\mathbf{E}_{\rm ac}(t)$ to the static field $\mathbf{E}_{\rm dc}$. The Hamiltonian

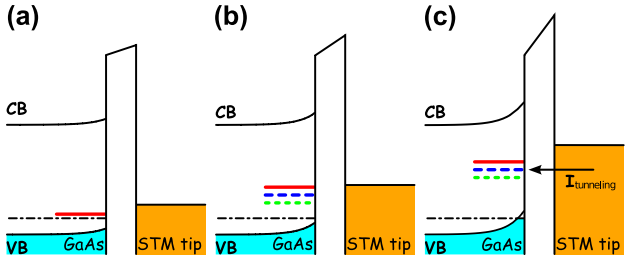

FIG. 3 (color online). Schematics of controlling the spin states via local band bending. The dotted-dashed lines show the chemical potential. The shaded regions are filled states. CB and VB label the conduction and valence bands of the semiconductor, respectively. (a) Initialization: For this voltage, occupation of the $|\xi_1\rangle$ state dominates. (b) Manipulation: Bring all the states into the gap but control the bias voltage below the threshold where the current starts to tunnel through these states. The oscillating field ($E_{\rm ac}$) drives transitions between the $|\xi_1\rangle$ and the $|\xi_2\rangle$ states. (c) Detection: Bring the final state further into the gap, so that electrons can tunnel from the tip into the acceptor state. The final state is identified according to the amplitude of the tunneling current [Fig. 2(d)].

$$\mathcal{H}_{\rm ESR} = \mathcal{H}_I(\mathbf{E}_{\rm dc}) + \mathcal{H}_I[\mathbf{E}_{\rm ac}(t)]. \quad (5)$$

To have a well-defined pseudospin 1/2, constructed out of $|\xi_1\rangle$ and $|\xi_2\rangle$, the coupling of these two states to $|\xi_3\rangle$ must vanish. For the schematic in Fig. 1, the oscillating field can be applied either along the [110] direction through the STM tip or along the [001] direction through the gates. Both choices leave $|\xi_3\rangle$ unaffected and only couple $|\xi_1\rangle$ and $|\xi_2\rangle$ to each other. To see how the states are coupled by the ac field, we write out $\mathcal{H}_I[\mathbf{E}_{\rm ac}(t)]$ using the eigenstates of $\mathcal{H}_I(\mathbf{E}_{\rm dc})$ as bases. We assume that the ac field $\mathbf{E}_{\rm ac}(t)$ is along the [110] direction.

$$\mathcal{H}_I[\mathbf{E}_{\rm ac}(t)] = \gamma E_{\rm ac}\cos(\omega t)\begin{pmatrix} -\sin 2\Theta & \cos 2\Theta & 0 \\ \cos 2\Theta & \sin 2\Theta & 0 \\ 0 & 0 & 0 \end{pmatrix}. \quad (6)$$

The off-diagonal term $\cos 2\Theta$, plotted in Fig. 2(c), shows how the coupling between the two coupled states changes with the field orientation. The coupling is maximized when the static field is completely along the [001] direction ($\theta = 0$). Then the static and oscillating electric fields are perpendicular to each other, just as the static and oscillating magnetic fields are perpendicular to each other in traditional ESR. In the limit $E_{\rm ac} \ll E_{\rm dc}$, the diagonal term can be neglected and our configuration works just like conventional ESR. The Rabi frequency obtained from the standard Rabi formula is

$$\hbar\,\Omega = \tfrac{1}{2}\sqrt{(\gamma E_{\rm ac}\cos 2\Theta)^2 + (\hbar\omega - \gamma E_{\rm dc}\sqrt{4-\cos^2\theta})^2}. \quad (7)$$

For $E_{\rm ac} = E_{\rm dc}/4 = 25$ kV/cm, and $\Theta = \pi/2$, $\Omega/2\pi =$ 12 GHz, corresponding to a Rabi time of 80 ps. Ensemble spin coherence times T_2^* measured by traditional ESR in GaMnAs exceed 0.5 ns (several times the estimated Rabi time) and appear due to the inhomogeneous environments of Mn ions [26]; the T_2's of individual spins are expected to be considerably longer. Hyperfine interactions, which significantly affect conduction electron spin coherence, are expected to be weak for Mn ions as the overlap of the valence p orbitals with the nucleus is small.

High-fidelity determination of the orientation of the pseudospin can be achieved by measuring the total tunneling current through the final state with the STM [9]. When the tip-sample voltage is increased, and the semiconductor bands bend further [see Fig. 3(c)], current starts to tunnel through the bound hole wave function state [27,29], and the tunneling current is proportional to the probability density of the state at the STM tip location. The spatial structure of these $J = 1$ states is highly anisotropic [24,27,29]. We calculate the two eigenstates to have the following spatial structure:

$$\langle \mathbf{r}|\xi_i\rangle = c_{XY}^i\langle \mathbf{r}|X+Y\rangle + c_Z^i\langle \mathbf{r}|Z\rangle, \quad (8)$$

where $c_{XY}^1 = \sin\Theta$, $c_{XY}^2 = -\cos\Theta$, and $|X+Y\rangle = (|X\rangle + |Y\rangle)/\sqrt{2}$. If the STM tip is positioned directly over the Mn

dopant, it probes the nodal plane, $\langle \mathbf{r}|Z\rangle = 0$. In this particular case, the local density of states (LDOS) is simply proportional to the projection on to the $\langle \mathbf{r}|X + Y\rangle$ state, which is $|\sin\Theta|^2$ for $|\xi_1\rangle$ and $|\cos\Theta|^2$ for $|\xi_2\rangle$. Thus, for a static electric field along $\theta = 0$ ($\Theta = \pi/2$) and the pseudospin in the $|\xi_2\rangle$ state, no current will be detected, but for the pseudospin in the $|\xi_1\rangle$ state there will be current detected. The difference in current for the $|\xi_1\rangle$ and $|\xi_2\rangle$ states is shown in Fig. 2(d). For this position, about 10% of the LDOS is not spin-dependent, which reduces maximum visibility to 90% (at, e.g., $\theta \approx 0$). Spatial averaging of the LDOS over a typical experimental 2 Å changes the visibility by only a few percent. The asymmetric angular dependence is due to the lack of inversion symmetry of the substituted ion in a tetrahedral host. Current measurement time scales can be very fast, as STM experiments performed at 50 GHz have demonstrated [30]. We also assume that the tunneling current is small so that spin flip does not occur during the measurement.

Controllable coupling of two spins permits use of these Mn ions for quantum information processing. Estimates of the overlap of holes bound to two separated Mn ions [24] indicate ~100 meV splittings of Mn pair states for ions separated by 12 Å along the $(1\bar{1}0)$ direction. The overlap falls off for larger separations according to the ~13 Å wave function radius [9] of the bound hole, so it would be ~0.1 meV for two ions 10 nm apart. This overlap could be reduced, increased, or eliminated with a gate between the two ions [14,15]. By using single Mn manipulations to put single ion quantum information in the proper pair of single Mn states, the Mn pair state splitting can be used to perform CNOT operations in an analogous way to how the singlet-triplet splitting is used for a CNOT with spin-1/2 qubits.

In conclusion, we have presented a concrete proposal for electrically initializing, manipulating, and detecting single pseudospin states of a magnetic dopant in a semiconductor. All-electrical spin manipulation should be possible for other impurities in tetrahedral semiconductors characterized by $J > 1/2$ ground state spins (e.g., most transition-metal ions in most tetrahedral semiconductors or the nitrogen-vacancy center in diamond). In a future scalable architecture, the STM tip would be replaced by a gate-controlled contact. The controlled resistance of that contact would permit alternation between the gate configuration for manipulation and the contact configuration for initialization and detection, all without moving parts. The [001] static electric field, here assumed to be implemented with gates, may also be replaced by an internal electric field from a doping gradient (such as in a $p - n$ junction), or even a static strain field. The Mn ions could be controllably placed within the surface relative to the contacts using current pulses from an STM tip as described in Ref. [23].

This work is supported by ARO MURI No. DAAD19-01-1-0541 and DARPA QuIST No. DAAD-19-01-1-0650.

[1] D. Rugar, R. Budakian, H. J. Mamin, and B. W. Chui, Nature (London) **430**, 329 (2004).
[2] M. Xiao, I. Martin, E. Yablonovitch, and H. W. Jiang, Nature (London) **430**, 435 (2004).
[3] A. Gruber *et al.*, Science **276**, 2012 (1997).
[4] F. Jelezko, I. Popa, A. Gruber, C. Tietz, J. Wrachtrup, A. Nizovtsev, and S. Kilin, Appl. Phys. Lett. **81**, 2160 (2002).
[5] Y. Manassen, R. J. Hamers, J. E. Demuth, and A. J. Castellano, Jr., Phys. Rev. Lett. **62**, 2531 (1989).
[6] C. Durkan and M. E. Welland, Appl. Phys. Lett. **80**, 458 (2002).
[7] A. J. Heinrich, J. A. Gupta, C. P. Lutz, and D. M. Eigler, Science **306**, 466 (2004).
[8] J. M. Elzerman *et al.*, Nature (London) **430**, 431 (2004).
[9] J.-M. Tang and M. E. Flatté, Phys. Rev. B **72**, 161315(R) (2005).
[10] G. Prinz, Science **282**, 1660 (1998).
[11] S. A. Wolf *et al.*, Science **294**, 1488 (2001).
[12] *Spin Electronics*, edited by M. Ziese and M. J. Thornton, Lecture Notes in Physics Vol. 569 (Springer-Verlag, Berlin, 2001).
[13] *Semiconductor Spintronics and Quantum Computation*, edited by D. D. Awschalom, N. Samarth, and D. Loss (Springer-Verlag, Berlin, 2002).
[14] D. Loss and D. P. DiVincenzo, Phys. Rev. A **57**, 120 (1998).
[15] B. E. Kane, Nature (London) **393**, 133 (1998).
[16] A. Imamoğlu *et al.*, Phys. Rev. Lett. **83**, 4204 (1999).
[17] C. E. Pryor and M. E. Flatté, quant-ph/0211160.
[18] G. F. Quinteiro and C. Piermarocchi, Phys. Rev. B **72**, 045334 (2005).
[19] Y. Kato, R. C. Myers, D. C. Driscoll, A. C. Gossard, J. Levy, and D. D. Awschalom, Science **299**, 1201 (2003).
[20] Y. K. Kato, R. C. Myers, A. C. Gossard, and D. D. Awschalom, Nature (London) **427**, 50 (2004).
[21] D. P. DiVincenzo, D. Bacon, J. Kempe, G. Burkard, and K. B. Whaley, Nature (London) **408**, 339 (2000).
[22] J. R. Petta *et al.*, Science **309**, 2180 (2005).
[23] D. Kitchen, A. Richardella, and A. Yazdani, J. Supercond. **18**, 23 (2005).
[24] J.-M. Tang and M. E. Flatté, Phys. Rev. Lett. **92**, 047201 (2004).
[25] T. C. Lee and W. W. Anderson, Solid State Commun. **2**, 265 (1964).
[26] J. Schneider, U. Kaufmann, W. Wilkening, M. Baeumler, and F. Köhl, Phys. Rev. Lett. **59**, 240 (1987).
[27] A. M. Yakunin *et al.*, Phys. Rev. Lett. **92**, 216806 (2004).
[28] P. I. Arseev, N. S. Maslova, V. I. Panov, S. V. Savinov, and C. van Haesendock, Pis'ma Zh. Eksp. Teor. Fiz. **77**, 202 (2003) [JETP Lett. **77**, 172 (2003)].
[29] A. M. Yakunin *et al.*, Physica (Amsterdam) **21E**, 947 (2004).
[30] G. M. Steeves, A. Y. Elezzabi, and M. R. Freeman, Appl. Phys. Lett. **72**, 504 (1998).